



HAL
open science

Functional versus phylogenetic fingerprint analyses for monitoring hydrogen-producing bacterial populations in dark fermentation cultures

Marianne Quéméneur, Jérôme Hamelin, Eric Latrille, Jean-Philippe Steyer,
Eric Trably

► To cite this version:

Marianne Quéméneur, Jérôme Hamelin, Eric Latrille, Jean-Philippe Steyer, Eric Trably. Functional versus phylogenetic fingerprint analyses for monitoring hydrogen-producing bacterial populations in dark fermentation cultures. *International Journal of Hydrogen Energy*, 2011, 36 (6), pp.3870 - 3879. 10.1016/j.ijhydene.2010.12.100 . hal-01809618

HAL Id: hal-01809618

<https://amu.hal.science/hal-01809618>

Submitted on 8 Aug 2023

HAL is a multi-disciplinary open access archive for the deposit and dissemination of scientific research documents, whether they are published or not. The documents may come from teaching and research institutions in France or abroad, or from public or private research centers.

L'archive ouverte pluridisciplinaire **HAL**, est destinée au dépôt et à la diffusion de documents scientifiques de niveau recherche, publiés ou non, émanant des établissements d'enseignement et de recherche français ou étrangers, des laboratoires publics ou privés.



Distributed under a Creative Commons Attribution - NonCommercial - NoDerivatives 4.0 International License

1 **Functional versus phylogenetic fingerprint analyses for monitoring**
2 **hydrogen-producing bacterial populations in dark fermentation cultures**

3

4

5

6

7 Marianne Quéméneur, Jérôme Hamelin, Eric Latrille, Jean-Philippe Steyer, and Eric Trably*

8

9

10 Author address:

11 INRA, UR050, Laboratoire de Biotechnologie de l'Environnement, avenue des Etangs,

12 Narbonne, F-11100, France

13

14

15 * Corresponding author:

16

17 Tel.: +33(0)468425151 ; Fax: +33(0)468425160 ; E-mail address: trably@supagro.inra.fr;

18

19 **Abstract**

20 The fermentative hydrogen production during the anaerobic digestion of organic matter is a
21 promising technology for the renewable energy search. However, the mixed culture
22 fermentation performances vary considerably depending on environmental conditions such as
23 pH. We investigated the ability of a molecular CE-SSCP (capillary electrophoresis-single
24 strand conformation polymorphism) fingerprinting method based on the *hydA* functional
25 genes to describe better the bacterial community dynamics, as compared to the standard 16S
26 rDNA-based method. A series of batch experiments was performed from sucrose at different
27 initial pH from 4 to 6. As expected, higher H₂ production potentials (H_{max}) and rates (R_{max})
28 were obtained at the highest pH. Changes in batch performances were associated with shifts
29 in the *hydA* diversity and structure. In contrast, 16S rDNA-based fingerprints were less
30 sensitive to changes in H₂ production performances. The H_{max} was related to lower *hydA*
31 diversity, with *Clostridium sporogenes* as the major H₂ producer. Communities harboring
32 larger *hydA* diversities were found in experiments with the higher R_{max}, suggesting that
33 species coexistence may have positive effects on H₂ productivity.

34

35 **Keywords**

36 Biohydrogen; 16S rDNA fingerprint; *hydA* functional genes; anaerobic digestion; mixed
37 cultures; microbial diversity.

38 **1. Introduction**

39

40 Dark fermentation using mixed anaerobic microbial communities is an attractive way to
41 produce hydrogen (H₂), one of the most promising clean and sustainable energy carriers [1,
42 2]. In recent years, the mixed microbial cultures have been investigated for producing H₂ at
43 low cost from renewable organic wastes [2, 3, 4]. With regard to pure cultures, mixed cultures
44 are more suitable for degrading a wide range of substrates, due to their better adaptation to
45 diverse media and their high resistance and resilience against environmental changes or
46 organic matter loads.

47 H₂ is a key metabolic intermediate used for electron carrier for interspecies energy transfer
48 exchanges in anoxic systems. Therefore, when environmental conditions change, the H₂
49 production performances observed in mixed cultures are not only affected by the metabolic
50 shifts, but also by the changes in population structures [5-7]. Indeed, the presence and activity
51 of efficient H₂-producing bacteria (HPB), in mixed cultures, can be strongly affected by the
52 metabolic and phylogenetic interactions between the different community members.
53 Consequently, a better understanding of the bacterial population dynamics is needed for
54 improving the stability and the performances of H₂ dark fermentation bioprocesses. These
55 bacterial population dynamics can be analyzed using different levels of resolution:
56 phylogenetic and/or functional. To this end, accurate molecular tools and descriptors have to
57 be used to gain insights into the links between diversity/structure of the bacterial community
58 and H₂ evolution.

59 For the past decade, the fingerprinting techniques based on 16S rDNA sequences have been
60 widely used to characterize the bacterial communities in H₂ dark fermentation processes [3, 5,
61 8-12]. These fingerprinting techniques, including denaturing gradient gel electrophoresis
62 (DGGE) [13], terminal restriction fragment length polymorphism analysis (T-RFLP) [14] or

63 capillary electrophoresis-single strand conformation polymorphism analysis (CE-SSCP) [15]
64 provide simultaneously: (i) a rapid analysis of the relative abundance of the different
65 community members; and (ii) a comparative analysis of the microbial population structures in
66 relation to the changes in environmental conditions. These fingerprinting techniques were
67 previously applied to identify the prominent species in HPB mixed cultures and to correlate
68 their presence to the H₂ production performances and the environmental conditions. In this
69 way, the highest H₂ production yields were usually observed when mixed cultures were
70 predominantly composed of *Clostridium* species [2, 4, 7]. The fingerprinting techniques are
71 well adapted for analyzing the microbial communities and investigating the inter-species
72 interactions in dark fermentation bioreactors, because H₂ production often relies on a
73 relatively small number of highly specialized microbial species. However, relatively little is
74 known about the relationship existing between the microbial community structure and the H₂
75 production performances. Methods based on 16S rDNA provide information about the
76 phylogeny of bacterial species present in the community, but not direct physiological
77 information and fail occasionally to distinguish closely related H₂-producing *Clostridium*
78 species [6, 16].

79 Regarding the overall 16S rDNA fingerprint methods, very few studies have specifically
80 characterized the HPB populations using functional fingerprinting methods [6, 11]. In
81 particular, the fingerprinting methods based on *hydA* genes, encoding the [Fe-Fe]-
82 hydrogenases (H₂ases) are very meaningful, as they specifically target the bacterial
83 populations directly involved in H₂ evolution, and provide valuable information about their
84 structure and diversity. Several methods are now available for evaluating and comparing the
85 fingerprint patterns [17-19]. Moreover, the diversity and dynamics of bacterial communities
86 can be quantified from CE-SSCP profiles, using molecular descriptors such as Simpson's
87 diversity index or Euclidean distances [20]. At last, if combined with multivariate analyses,

88 they can be used to find statistical correlations between the microbial community structures
89 and the environmental parameters [20, 21]. Many environmental parameters can change the
90 performance of fermentative H₂ production by modifying the bacterial metabolic pathways
91 and community structure [2, 4, 7]. Among them, the pH appears to be one of the most
92 important factor influencing H₂ performances [4, 22, 23]. The pH also influences the
93 microbial community structure because it is a key parameter affecting carbon metabolism and
94 growth rates of microorganisms [12].

95 In this paper, both *hydA*- and 16S rRNA gene-based fingerprinting methods were compared
96 for monitoring bacterial population dynamics in response to pH changes. A series of batch
97 tests were operated at different initial pH to induce a wide range of H₂ production
98 performances and different bacterial composition. The fingerprint characterization followed
99 by identification of H₂ producers were also used to assess link between H₂ production
100 performances and bacterial community structures and diversities.

101

102 **2. Materials and methods**

103

104 **2.1. Hydrogen production in batch tests**

105

106 The H₂ production experiments were carried out in 500 mL glass bottles under batch
107 conditions. The inoculum corresponded to an anaerobically digested sludge pretreated by
108 heat/shock treatment (90°C, 10 min). Two milliliters of the pretreated inoculum (final
109 concentration of 225 mg-COD/L) were inoculated in the following culture medium: 40 mM
110 MES, 10 g sucrose, 1L deionized water. The total working volume was 200 mL. The initial
111 pH was adjusted to 4, 4.5, 5, 5.5 and 6. All batch tests were performed in triplicates. After
112 inoculation, each bottle was flushed with nitrogen for 5 min to maintain anaerobic conditions.

113 The bottles were then capped with a rubber stopper and incubated at 37°C for 24 days. Four
114 milliliters of the mixed cultures were collected daily during the first 10 days of the
115 experiments, and every 2nd-3rd day during the last 14 days of the experiments. The samples
116 were centrifuged (20,000 g, 10 min) and the supernatants and the pellets were stored at -20°C
117 for further chemical analyses and DNA extraction, respectively.

118

119 **2.2. Chemical analysis (biogas, metabolic byproducts)**

120

121 The volume of biogas was daily measured using an acidified water displacement method. The
122 biogas composition (CH₄, CO₂, H₂ and N₂) was determined by gas chromatography (GC-14A,
123 Shimadzu) as previously described by Aceves-Lara *et al.* [23].

124 The volatile fatty acids (VFA) composition in the liquid phase, *i.e.* acetic acid (C₂), propionic
125 acid (C₃), butyric and iso-butyric acids (C₄ and iC₄) and valeric and iso-valeric acids (C₅ and
126 iC₅), were determined by gas chromatography coupled to catharometric detection (GC 8000,
127 Fisons Instruments). The concentrations of sugars and non-VFAs metabolic byproducts, such
128 as organic acids (lactate), ethanol or acetone were assessed by High Performance Liquid
129 Chromatography analysis coupled to a refractometer (Waters Assoc.). The substrate
130 degradation efficiency was estimated by dividing the amount of sucrose consumed by the
131 amount of initial sucrose. The H₂ production performances were characterized with the
132 following parameters, as described by Quéméneur *et al.* [6]: H₂ production potential (mL/L or
133 mmol-H₂/L), H₂ production rates (mmol-H₂/L/d) and H₂ production yield (mol-H₂/mol-
134 hexose-consumed). The H₂ production potential (H) was the cumulative H₂ production. The
135 H₂ production rate (R) represented the daily H₂ production increase. The H₂ yield was
136 calculated by dividing the maximum H₂ production potential by the sucrose consumed.

137

138 **2.3. DNA extraction and PCR amplification**

139

140 For each experiment, molecular analyses of the bacterial communities were performed on the
141 triplicate samples at the start of the experiments (initial time), at the maximum H₂ production
142 rate (R_{max}), at the maximum H₂ production potential (H_{max}) and at the end of the experiments
143 (after 24-day incubation).

144 Genomic DNA was extracted and purified from cell pellets using the Wizard Genomic DNA
145 Purification kit (Promega). The purity and amount of DNA in the extracts were measured by
146 spectrophotometry (Infinite NanoQuant M200, Tecan).

147 The *hydA* genes were amplified using two non-degenerated primers, *hydAClosF* (5' –
148 ACCGGTGGAGTTATGGAAGC – 3', *C. pasteurianum* position F1258) and 5'-fluorescein
149 phosphoramidite-labeled *hydAClosR* (5' – CATCCACCTGGACATGCCAT – 3', *C.*
150 *pasteurianum* position R1508), designed from two consensus regions of an alignment of 31
151 *hydA Clostridium* reference sequences [6]. Each PCR mixture (50 µL) contained 1X *Pfu*
152 Turbo DNA polymerase buffer, 200 µM of each dNTP, 0.5 µM of each primer, 0.5 U of *Pfu*
153 Turbo DNA polymerase (Stratagene) and 10 ng of genomic DNA. Reactions were performed
154 in a Mastercycler thermal cycler (Eppendorf). The *hydA* genes were amplified as follows:
155 94 °C for 2 min, followed by 35 cycles of 94 °C for 30 s, 57 °C for 30 s, and 72 °C for 30 s,
156 with a final extension at 72 °C for 10 min. The presence and size of about 200 bp PCR
157 products were determined by ethidium bromide-stained (2%) gel electrophoresis.

158 Meanwhile, the 16S rRNA genes were amplified using *Pfu* Turbo DNA polymerase
159 (Stratagene) and universal primers W49 (5'-ACGGTCCAGACTCCTACGGG-3', *Escherichia*
160 *coli* position F331) [24] and 5'-fluorescein phosphoramidite-labeled W104 (5'-
161 TTACCGCGGCTGCTGGCAC-3', *E. coli* position R533) [24], targeting about 200 bp of the
162 V3 region of the 16S rRNA gene. The PCR reactions were performed as described above,

163 except that 25 cycles and primer hybridization at 61 °C were applied and 130 ng of each
164 primer were used. The *Clostridium* genus was specifically analyzed by nested PCR. First, the
165 16S rRNA genes of the *Clostridium* genus were amplified using AccuPrime *Taq* DNA
166 polymerase (Invitrogen), a bacterial domain forward primer W18 (5'-
167 GAGTTTGATCMTGGCTCAG -3', *E. coli* position F9) [15] and a *Clostridium*-specific
168 reverse primer W109 (5'- CCCTTTACACCCAGTAA -3', *E. coli* position R561) [25], as
169 described by Peu *et al.* [26]. Then, the diluted PCR products was used as a template for a
170 universal 16S rDNA PCR, carried out using the primer set W49/W104.

171

172 **2.4. CE-SSCP electrophoresis and statistical analyses**

173

174 One microliter of 5- to 2000-fold diluted PCR product was mixed with 18.8 µL of formamide
175 and 0.2 µL of internal standard GeneScan ROX (Applied Biosystems). Samples were heat-
176 denatured at 95°C for 5 min and immediately cooled in ice. CE-SSCP electrophoresis was
177 performed in an ABI Prism 3130 genetic analyser (Applied Biosystems) with 50 cm-long
178 capillary tubes filled with a non-denaturing 5.6% conformation analysis polymer (Applied
179 Biosystems). Samples were eluted at 12 kV and 32°C for 30 min (for 16S rRNA gene) or 64
180 min (for *hydA* gene). Raw CE-SSCP data were analyzed using GeneScan software (Applied
181 Biosystems).

182 The CE-SSCP profiles were aligned with the internal standard ROX to correct any change in
183 the electrophoretic motility between runs. The sum of the peak areas were normalized to unit
184 before statistical analysis. The StatFingerprints library from R was used (R Development
185 Core Team 2009) [27]. Euclidean Distances (ED) between each pair of CE-SSCP profiles
186 were calculated for matrix generation and used as measurements of dissimilarity between
187 bacterial communities.

188 An analysis of similarity (ANOSIM) was also used to investigate the effects of the initial pH,
189 considered as a qualitative variable, on the structure of bacterial communities [28]. ANOSIM
190 gives a statistic, ANOSIM R, which indicates the magnitude of dissimilarities among groups
191 of samples. An ANOSIM R = 1 indicates that the groups of communities with different initial
192 pH are dissimilar, and at the opposite, ANOSIM R = 0 indicates that the groups cannot be
193 distinguished statistically. The statistical significance of ANOSIM R was tested by Monte
194 Carlo randomization.

195 ED were also used to compare, over time, the effect of the initial pH on the divergence of the
196 bacterial communities at functional (*hydA* genes) and phylogenetic levels (16S rRNA genes).
197 For each batch tests, the ED was normalized by dividing the values obtained at each time by
198 the largest distance calculated for the time course, giving values between 0 and 1 during the
199 24-day incubations. A normalized ED = 1 means that the community is the most dissimilar to
200 that on day 0 and a normalized ED = 0 means that the community is identical to that on day 0.
201 The complexity of the bacterial community was estimated using Simpson's diversity index
202 (D) from a CE-SSCP profile, by considering the number of species (number of peaks) as well
203 as their relative abundance (area under each peak) [29].

204

205 **2.5. Assignment of the partial *hydA* sequences in mixed cultures**

206

207 The PCR products obtained from the H₂-producing mixed cultures were purified using a PCR
208 Purification Kit (Qiagen). The *hydA* clone libraries were constructed using the TA Cloning kit
209 (Invitrogen). The PCR-CE-SSCP profile of each PCR product, amplified using plasmid-
210 targeted primers T7 and P13, was compared with the HPB culture profiles for peak
211 assignment. The cloned inserts were sent for sequencing (MilleGen company, Toulouse,
212 France). The protein sequences, deduced from the nucleotide *hydA* sequences, were aligned

213 with reference sequences retrieved from the Genbank database using the CLUSTALW
214 program [30], and further refined manually using the BioEdit program [31]. Distances were
215 estimated by the Kimura method [32], and the neighbor-joining method was used for inferring
216 the tree topologies [33]. Tree topology confidence was determined by bootstrap analysis on
217 1000 replicates [34]. All phylogenetic programs were implemented with SeaView software
218 [35]. The *hydA* gene sequences were deposited in the Genbank database under the accession
219 numbers HQ241275 to HQ241278.

220

221 **3. Results and discussion**

222

223 **3.1. Hydrogen production in batch tests**

224

225 The biogas produced by mixed cultures contained only H₂ and CO₂, without detectable CH₄,
226 suggesting that the heat shock pretreatment was effective for inhibiting the methanogenic
227 bacteria issued from the anaerobic sludge.

228 Figure 1 shows the accumulated H₂ production in mixed cultures at different initial pH over
229 the 24 days of incubation. Table 1 summarizes the results of pH experiments. In comparison
230 with other reports [12, 36, 38], time to reach the higher cumulated H₂ is large (ranging
231 between 9.7 and 24 days) because the nutrients (except carbon source) were just provided by
232 the inoculum. The maximal H₂ production rates (R_{\max}) increased gradually from 16.4 to 38.3
233 mmol-H₂/L/d with the increase in pH from pH 4 to 6 ($p < 0.05$). Initial pH also affected H₂
234 production with the highest maximum H₂ production (H_{\max}) of 102.7 mmol-H₂/L attained at
235 pH 5 ($p < 0.05$). Indeed, the H_{\max} increased with the rise in pH from 4 to 5, but reached a level
236 of equilibrium in the pH range from 5 to 6 (Table 1). It is noteworthy that the H_{\max} obtained at
237 pH 5.5 and pH 6 were reached earlier than pH 5, indicating that higher pH improves H₂

238 production reaction. Interestingly, at pH 5.5 and pH 6, the H₂ production phase was followed
239 by H₂ consumption phase (Figure 1). The H₂ content in the gas phase increased until the H_{max}
240 was reached (44.5% and 43.3%, for pH 5.5 and pH 6 respectively), and then declined at the
241 end of experiments (28.5% and 27.4%, respectively) (Table 1). Similar H₂ consumption
242 phases have previously been reported during fermentative H₂ production batch tests [36, 37].
243 The present results showed that the optimal pH for H₂ production was in the range of 5 to 6.
244 They were in agreement with comparable studies (*i.e.* batch cultures, without pH control,
245 using 10 g-sucrose/L and heat-shocked mixed microflora) [38, 39]. For instance, Van Ginkel
246 *et al.* [39] studied H₂ production in a pH range 4.5-6.5, using compost, potato soil or soybean
247 soil as seed microflora, and found that pH 5-6 were the most suitable for H₂ production.
248 Khanal *et al.* [38] studied H₂ production in a pH range 4.5-6.5 using compost, and showed
249 that higher R_{max} were obtained at higher pH. Shorter duration of the H₂ production was also
250 found at higher pH and final pH increased with the increase in initial pH (Table 1). However,
251 our results were different from this latter study [38], because these authors found the highest
252 H_{max} at pH 4.5. A low pH 4.5 was also found optimal for H₂ production in a pH range 4-7
253 using anaerobic digester sludge [12]. In our study, no significant difference was observed
254 between the H₂ yields ranging between 1.7 and 2 mol-H₂/mol-hexose (Table 1). This finding
255 can be explained by the variation of the substrate degradation efficiency increasing from
256 53.4% to 100% with the increase in pH (Table 1). H₂ yield of 2 mol-H₂/mol-hexose
257 associated with optimal pH 5.5-6 were previously obtained using mixed cultures [40] or pure
258 cultures [41].

259 As expected, the cumulated H₂ production was strongly correlated to intermediate metabolite
260 productions (Table 1). The gradual increase of R_{max} in the pH range from 4 to 6 matched with
261 the increase in intermediate metabolites. The productions of total VFAs and overall soluble
262 microbial products (SMPs) also increased with the increase of H_{max} in the pH range from 4 to

263 5, but achieved a level of equilibrium within pH range 5 to 6 (Table 1). When H_{\max} was
264 reached, butyrate (Bu) and acetate (Ac) contents in the SMPs ranged from 63.0% to 72.3%
265 and 25.3% to 27.7%, respectively, while ethanol constituted only 5.6 to 11.5%. The
266 production of Bu and Ac, as the major fermentation products, suggested that *Clostridium*
267 species were the dominant bacteria in the mixed cultures. No significant difference of Bu/Ac
268 ratios, ranging between 2.5 and 2.7, were detected according to pH (Table 1), suggesting that
269 no metabolic switches occurred when H_{\max} was reached. At the end of the experiment, after
270 the H_2 consumption phase, at pH 5.5 and pH 6, caproate accumulated and represented 4.0%
271 and 6.1% of the SMPs, respectively. Moreover, at pH 5.5 and pH 6, Bu/Ac ratios decreased
272 significantly from 2.7 and 2.5 to 1.8 and 2.1, respectively. The H_2 consumption phase can
273 result from two metabolic pathways, either homoacetogenesis, producing only acetate from
274 H_2 and CO_2 , and caproate formation, produced from H_2 and equimolar acetate and butyrate.
275 Such changes in Bu/Ac ratios can be explained by metabolic alterations or switches due to
276 environmental changes such as pH [38], but also can result from microbial community
277 structure shifts during the fermentative H_2 production.

278

279 **3.2. Functional and phylogenetic dynamics of the bacterial community**

280

281 CE-SSCP fingerprinting was used to compare the bacterial community structures at various
282 pHs. Whatever the initial pH, highly similar bacterial- and *Clostridium*-specific 16S rDNA
283 CE-SSCP fingerprinting patterns were obtained from all the H_2 -producing cultures (data not
284 shown). This result indicated that the *Clostridium* genus was largely dominant and played a
285 key role in these H_2 -producing experiments. This finding suggested that the use of a heat-
286 shock pretreated sludge as inoculum led to select a large majority of *Clostridium* species as
287 already mentioned in previous studies [4-7].

288 Figure 2 represents the relative divergence of the bacterial communities over time in response
289 to the pH changes. Whatever the gene tested, the highest changes in CE-SSCP profiles were
290 observed during the first days of the experiments when R_{\max} was reached. The divergence
291 gradually increased with decreasing pH. Moreover, the highest increase of the community
292 divergence was obtained at pH 4 between day 3 and 6 and the lowest was at pH 6. It is
293 noteworthy to say that R_{\max} was the lowest at pH 4 and the highest at pH 6 (Table 1). For all
294 pH, the maximal relative divergences were observed after 10 days of experiment. At pH 4-5,
295 the relative divergence was stable until the end of the experiments. In contrast, at pH 5.5 and
296 6, a decrease in the relative divergence was shown at day 24, when H_2 consumption was
297 observed (Figure 1). Thus, the shift of the CE-SSCP profiles over time was correlated to the
298 pH changes. Fang *et al.* [12] also showed that total bacterial community structure changed
299 with respect to pH changes. However, our study showed that the *hydA* structure was globally
300 more affected by the pH than the total bacteria population structure (*hydA* ANOSIM $R = 0.29$,
301 $p < 0.001$; 16S rDNA ANOSIM $R = 0.16$, $p < 0.05$). In addition, high initial relative
302 divergences were observed for the *hydA* profiles, indicating a more sensitive response of the
303 HPB population to the pH changes. Moreover, contrary to 16S rDNA structure, significant
304 negative correlation was also observed between R_{\max} and the rate of *hydA* structure change.
305 Consequently, our results indicated that the changes in the *hydA* community structure
306 provided better information to monitor H_2 production change than the total bacteria
307 population structure.

308 Figure 3 shows, for each pH, the dynamics of the CE-SSCP fingerprints based on the *hydA*
309 (Figure 3A) and 16S rRNA genes (Figure 3B) over the 24-day incubations. Both the *hydA* and
310 16S rDNA CE-SSCP profiles showed pattern succession consisting of a simplification phase
311 followed by stabilization and/or instability phase. This simplification was slower at high pH,
312 and thus, at high R_{\max} . At the R_{\max} time, after 3 days (6 days in the case of pH 4), the gradual

313 disappearance of CE-SSCP peaks in relation to pH led to highest dissimilarities within the
314 CE-SSCP profiles. At the H_{\max} time (day 10 for pH 5.5-6 and day 24 for pH 4-5), the CE-
315 SSCP fingerprints were both composed of only one major peak and several minor peaks.
316 Interestingly, additional peaks appeared in CE-SSCP profiles at pH 5.5 and 6, at 24 days,
317 when H_2 consumption occurred. As previously observed [5, 6], the appearance and
318 disappearance of CE-SSCP peaks, reflecting changes in the bacterial community composition,
319 was correlated to H_2 production performances. A simplification followed by a stabilization of
320 the total bacterial communities have also been reported in similar batch tests of fermentative
321 H_2 production [12] or photo- H_2 production [42]. These authors made the assumption that after
322 a process of competition or cooperation, during the first days, the bacterial community
323 structure tended to be stable for forming an optimal HPB population before H_{\max} [10]. Our
324 results were in agreement with the occurrence of such competition/cooperation processes. In
325 addition, our findings were also consistent with previous studies showing that *hydA*
326 population structure shifted over time [11, 43]. As *hydA* structure was correlated to H_2 content
327 shift, Tolvanen *et al.* [43] have reported that *hydA* qPCR melting curve analysis could be used
328 as an indicator of H_2 performance. Nevertheless, these authors have also indicated that
329 fingerprinting techniques, such as DGGE or CE-SSCP, provide better resolution than qPCR
330 melting curves for distinguishing different genes [43]. In this study, the *hydA* structure
331 obtained by CE-SSCP analysis was thus a more reliable and functional tool for monitoring
332 bioreactor performances. Moreover, this *hydA* functional fingerprint analysis was also more
333 suitable than 16S rDNA fingerprint analysis for monitoring HPB populations in dark
334 fermentation cultures.

335

336 **3.3. Bacterial population diversities**

337

338 Simpson's diversity indices (D) were calculated to assess the complexity of the CE-SSCP
339 profiles and to compare the diversity of the H₂-producing and total bacterial communities
340 cultivated at different initial pH. Simpson's diversity index (D) corresponds to the probability
341 that two individuals randomly selected from a community belong to the same species [29].
342 Figure 4 presents the D values obtained from the *hydA* and 16S rDNA CE-SSCP profiles
343 when the R_{max} (Figure 4A) and the H_{max} (Figure 4B) were reached. The D values obtained
344 from the 16S rDNA CE-SSCP profiles were higher than those obtained from the *hydA* CE-
345 SSCP profiles (Figures 4A and 4B). Whatever the gene tested the lowest D values were
346 observed when the H_{max} occurred (Figure 4B), while the highest values were obtained at the
347 R_{max} (Figure 4A). These results were in agreement with previous studies showing that the
348 H_{max} was associated with low bacterial diversity.

349 When H_{max} was reached, no significant difference was observed between the D values
350 obtained at different pH (Figures 4B). However, Fang *et al.* has reported that diversity
351 obtained at the H_{max} time increased with the rise of pH from 4.5 to 6.5 in an earlier study
352 carried out using anaerobic digested sludge as the inoculum and rice slurry as the substrate
353 (5.5 g-carbohydrate/L) [12]. This apparent difference is not contradictory with our results,
354 because similar results could be obtained if these authors had used twice as much sugar as in
355 our experience. Indeed, our results showed that the simplification of bacterial population was
356 slower at higher pH (Figures 2 and 3).

357 When R_{max} was reached, the *hydA* D values of the HPB communities ranged between 1.55
358 and 2.67 and increased significantly with the increase in pH ($p < 0.05$) (Figure 4A). The
359 lowest D value was observed at pH 4, and was related to the lowest R_{max}. In contrast, the
360 highest D value observed at pH 6 was related to the highest R_{max}. Correlation analysis
361 highlighted strong positive correlation between the R_{max} and the *hydA* D values. Thus, the
362 present results indicated that greater *hydA* diversity (*i.e.* a slower simplification of the HPB

363 population) leads to higher R_{\max} , suggesting the establishment of positive bacterial
364 interactions, such as co-metabolism or synergy. However, on a longer term, high *hydA*
365 diversity, as observed at pH 5.5 and 6, affected the stability of the highest cumulated H_2
366 production value (H_{\max}), through the increase in the H_2 consumption activity. Similarly, the
367 lowest 16S rDNA D value was found at the lowest pH while the highest D value was detected
368 at the highest pH 6 (Figure 4A). Nevertheless, contrary to the *hydA* diversity, no significant
369 correlation was found between 16S rDNA D values and the R_{\max} . Since the ecosystem
370 functionality correlated with the *hydA* diversity, it can be concluded that the *hydA* functional
371 marker was more informative than 16 rDNA phylogenetic marker and can be used as an
372 indicator of the H_2 production.

373

374 **3.4. Affiliation of hydrogen producers**

375

376 Five dominant *hydA* CE-SSCP peaks were detected during the 24 days incubation (Figure 3).
377 All peaks were assigned to *hydA* sequences affiliated with those of *Clostridium* cluster I
378 species (Figure 5), supporting the predominant role of this cluster in HPB mixed cultures [5,
379 16].

380 During the first days of the experiments and according to pH, from one to four different peaks
381 were detected within the *hydA* CE-SSCP profiles. Peaks 1-3 were detected in both pH 5.5 and
382 6 but were undetectable at lower pH. At pH 5.5 and 6, they were dominant after 3 days, when
383 R_{\max} was reached, but undetectable after 10 days, when H_{\max} occurred. The three *HydA*
384 sequence of clone that matched with peaks 1-3 formed a group showing 86.2-87.5 % identity
385 with that of *C. acetobutylicum* (Figure 5). Consequently, the increase of R_{\max} at highest pH
386 (Table 1) may be associated with the growth of *C. acetobutylicum hydA* like gene-carrying
387 strains known to be efficient H_2 producers at pH higher than 5.5 in pure cultures [41, 44].

388 Peak 4 was observed whatever pH and time, showing a wider ecological niche compared to
389 the other species of the seed inoculum. It dominated the *hydA* CE-SSCP at pH 4-5 and
390 became the dominant H₂ producer after 10 days at pH 5.5 and 6. The HydA sequence of the
391 clone matching with the peak 4 was affiliated with that of *Clostridium sporogenes* (70%
392 identity) (Figure 5) whose optimum growth pH is around 6-7. HydA sequences affiliated to *C.*
393 *sporogenes* were previously retrieved from mesophilic fermentative H₂-producing batch
394 cultures [6, 8]. In mesophilic continuous flow reactors using sucrose and heat-pretreated
395 inocula, Duangmanee *et al.* [45] also found *C. sporogenes* among other strains as dominant
396 species during H₂ production. This result confirms the key role of this species in H₂-producing
397 mixed cultures. Several studies with pure cultures of *C. sporogenes*, known as a non-toxicogenic
398 variant of *C. botulinum*, have been previously conducted to inhibit growth of the toxicogenic
399 species in food ecosystems [46]. However, to date no study has investigated biochemical
400 kinetics of fermentative H₂ production by *C. sporogenes*, despite its repeated detection in H₂-
401 producing mixed cultures. Future studies should investigate this aspect in more detail.

402 Peak 5 was only detectable during the H₂ consumption phase at pH 5.5 and 6, suggesting that
403 it could represent an H₂ consumer. Indeed, H₂ consumers, such as homoacetogens (*e.g.* *C.*
404 *carboxidivorans*, *C. magnum*), can also contain *hydA* genes and their presence could explain
405 the increase in acetate level at 24 days at pH 5.5 and 6. However, the HydA sequence of the
406 clone matching with the peak 5 exhibited 88.2% identity with that of *C. acetobutylicum*
407 (Figure 5), which has not yet been reported as
408 homoacetogen. However, the clostridial *hydA* database needs to be improved for obtaining
409 more accurate affiliation of clostridial H₂-producers in dark fermentative bioreactors. It is
410 noteworthy that the estimation of the clostridial strain function can be biased because
411 clostridial fermenters and homoacetogens are phylogenetically closely related [47].
412 Furthermore, some members of *Clostridium* genus, such as *C. acetobutylicum* or *C.*

413 *sporogenes*, detected during the H₂ consumption phase, are also known to harbor plasmid or
414 chromosomal genes encoding [NiFe]-H₂ases [48, 49]. Contrary to [FeFe]-H₂ases, [NiFe]-
415 H₂ases from *Proteobacteria* are usually known to catalyze H₂ uptake in vivo, but [NiFe]-
416 H₂ases from *Clostridia* have not yet been studied and there is no information about their
417 physiological function [48, 49]. Because this study focused on HPB, only clostridial genes
418 encoding [FeFe]-H₂ases have been targeted by specific functional primers [6]. Further
419 functional studies on both [Fe-Fe]- and [NiFe]-H₂ases have to be performed to investigate the
420 potential metabolic flexibility of *Clostridia* and the H₂ recycling in dark fermentation
421 processes.

422

423 **4. Conclusion**

424

425 In this study, the changes in both the taxonomic and functional bacterial community dynamics
426 were compared during fermentative H₂ production. The main result of this work was that
427 changes in *hydA* functional CE-SSCP fingerprints were better related to the H₂ production
428 performances than 16S rDNA patterns. This work also demonstrated the usefulness of
429 molecular descriptors, such as Simpson's diversity index and Euclidean distance, to visualize
430 changes in bacterial community in relation to changes in environmental factors. Like the
431 analysis of *hydA* gene expressions, the use of *hydA* fingerprinting CE-SSCP method coupled
432 with the estimation of molecular descriptors offers valuable information for improving dark
433 fermentation system monitoring and thus, provides a valuable tool for further studies on
434 bacterial interactions in fermentative H₂-producing bioreactors.

435

436 **Acknowledgement**

437

438 We gratefully acknowledge the financial support given for this research by the 'Institut
439 National de la Recherche Agronomique' (INRA). This work was funded by the InGEcoH
440 Project from the French National Research Agency (ANR) (ANR contract number 2008-
441 BIOE-005-01).

442 **References**

443

444 [1] Hallenbeck PC. Fermentative hydrogen production: Principles, progress, and
445 prognosis. *Int J Hydrogen Energy* 2009;34(17):7379-89.

446 [2] Hawkes FR, Hussy I, Kyazze G, Dinsdale R, Hawkes DL. Continuous dark
447 fermentative hydrogen production by mesophilic microflora: Principles and progress.
448 *Int J Hydrogen Energy* 2007;32(2):172-84.

449 [3] Davila-Vazquez G, Cota-Navarro CB, Rosales-Colunga LM, de Leon-Rodriguez A,
450 Razo-Flores E. Continuous biohydrogen production using cheese whey: Improving the
451 hydrogen production rate. *Int J Hydrogen Energy* 2009;34(10):4296-304.

452 [4] Wang JL, Wan W. Factors influencing fermentative hydrogen production: A review.
453 *Int J Hydrogen Energy* 2009;34(2):799-811.

454 [5] Huang Y, Zong WM, Yan X, Wang RF, Hemme CL, Zhou JZ, Zhou ZH. Succession
455 of the bacterial community and dynamics of hydrogen producers in a hydrogen-
456 producing bioreactor. *Appl Environ Microbiol* 2010;76(10):3387-90.

457 [6] Quéméneur M, Hamelin J, Latrille E, Steyer J-P, Trably E. Development and
458 application of a functional CE-SSCP fingerprinting method based on [Fe-Fe]-
459 hydrogenase genes for monitoring hydrogen-producing *Clostridium* in mixed cultures.
460 *Int J Hydrogen Energy* 2010; doi:10.1016/j.ijhydene.2010.07.076

461 [7] Valdez-Vazquez I, Poggi-Varaldo HM. Hydrogen production by fermentative
462 consortia. *Renew Sust Energy Rev* 2009;13(5):1000-13.

463 [8] Chang JJ, Chen WE, Shih SY, Yu SJ, Lay JJ, Wen FS, Huang CC. Molecular
464 detection of the clostridia in an anaerobic biohydrogen fermentation system by
465 hydrogenase mRNA-targeted reverse transcription-PCR. *Appl Microbiol Biotechnol*
466 2006;70(5):598-604.

- 467 [9] Chang JJ, Wu JH, Wen FS, Hung KY, Chen YT, Hsiao CL, Lin CY, Huang CC.
468 Molecular, monitoring of microbes in a continuous hydrogen-producing system with
469 different hydraulic retention time. *Int J Hydrogen Energy* 2008;33(5):1579-85.
- 470 [10] Xing DF, Ren NQ, Gong ML, Li JZ, Li QB. Monitoring of microbial community
471 structure and succession in the biohydrogen production reactor by denaturing gradient
472 gel electrophoresis (DGGE). *Science in China Series C-Life Sciences* 2005;48(2):155-
473 62.
- 474 [11] Xing DF, Ren NQ, Rittmann BE. Genetic diversity of hydrogen-producing bacteria in
475 an acidophilic ethanol-H₂-coproducing system, analyzed using the Fe-hydrogenase
476 gene. *Appl Environ Microbiol* 2008;74(4):1232-9.
- 477 [12] Fang HHP, Li CL, Zhang T. Acidophilic biohydrogen production from rice slurry. *Int*
478 *J Hydrogen Energy* 2006;31(6):683-92.
- 479 [13] Muyzer G, Dewaal EC, Uitterlinden AG. Profiling of complex microbial-populations
480 by denaturing gradient gel-electrophoresis analysis of polymerase chain reaction-
481 amplified genes-coding for 16S ribosomal-RNA. *Appl Environ Microbiol*
482 1993;59(3):695-700.
- 483 [14] Liu WT, Marsh TL, Cheng H, Forney LJ. Characterization of microbial diversity by
484 determining terminal restriction fragment length polymorphisms of genes encoding
485 16S rRNA. *Appl Environ Microbiol* 1997;63(11):4516-22.
- 486 [15] Lee DH, Zo YG, Kim SJ. Nonradioactive method to study genetic profiles of natural
487 bacterial communities by PCR-single-strand-conformation polymorphism. *Appl*
488 *Environ Microbiol* 1996;62(9):3112-20.
- 489 [16] Hung CH, Cheng CH, Cheng LH, Liang CM, Lin CY. Application of *Clostridium*-
490 specific PCR primers on the analysis of dark fermentation hydrogen-producing
491 bacterial community. *Int J Hydrogen Energy* 2008;33(5):1586-92.

- 492 [17] Fromin N, Hamelin J, Tarnawski S, Roesti D, Jourdain-Miserez K, Forestier N,
493 Teyssier-Cuvelle S, Gillet F, Aragno M, Rossi P. Statistical analysis of denaturing gel
494 electrophoresis (DGE) fingerprinting patterns. *Environ Microbiol* 2002;4(11):634-43.
- 495 [18] Marzorati M, Wittebolle L, Boon N, Daffonchio D, Verstraete W. How to get more
496 out of molecular fingerprints: practical tools for microbial ecology. *Environ Microbiol*
497 2008;10(6):1571-81.
- 498 [19] Ramette A. Multivariate analyses in microbial ecology. *FEMS Microbiol Ecol*
499 2007;62(2):142-60.
- 500 [20] Michelland RJ, Monteils V, Zened A, Combes S, Cauquil L, Gidenne T, Hamelin J,
501 Fortun-Lamothe L. Spatial and temporal variations of the bacterial community in the
502 bovine digestive tract. *J Appl Microbiol* 2009;107:1642-50.
- 503 [21] Lejon DPH, Nowak V, Bouko S, Pascault N, Mougél C, Martins JMF, Ranjard L.
504 Fingerprinting and diversity of bacterial *copA* genes in response to soil types, soil
505 organic status and copper contamination. *FEMS Microbiol Ecol* 2007;61(3):424-37.
- 506 [22] Fang F, Zeng RJ, Sheng GP, Yu HQ. An integrated approach to identify the influential
507 priority of the factors governing anaerobic H₂ production by mixed cultures. *Water*
508 *Res* 2010;44(10):3234-42.
- 509 [23] Aceves-Lara CA, Latrille E, Buffiere P, Bernet N, Steyer JP. Experimental
510 determination by principal component analysis of a reaction pathway of biohydrogen
511 production by anaerobic fermentation. *Chem Eng Process* 2008;47(11):1968-75.
- 512 [24] Delbes C, Moletta R, Godon JJ. Bacterial and archaeal 16S rDNA and 16S rRNA
513 dynamics during an acetate crisis in an anaerobic digester ecosystem. *FEMS*
514 *Microbiol Ecol* 2001;35(1):19-26.

- 515 [25] Van Dyke MI, McCarthy AJ. Molecular biological detection and characterization of
516 *Clostridium* populations in municipal landfill sites. Appl Environ Microbiol
517 2002;68(4):2049-53.
- 518 [26] Peu P, Brugere H, Pourcher AM, Kerouredan M, Godon JJ, Delgenes JP, Dabert P.
519 Dynamics of a pig slurry microbial community during anaerobic storage and
520 management. Appl Environ Microbiol 2006;72(5):3578-85.
- 521 [27] Michelland RJ, Dejean S, Combes S, Fortun-Lamothe L, Cauquil L. StatFingerprints:
522 a friendly graphical interface program for processing and analysis of microbial
523 fingerprint profiles. Mol Ecol Resour 2009;9(5):1359-63.
- 524 [28] Clarke KR. Nonparametric multivariate analyses of changes in community structure.
525 Aust J Ecol 1993;18(1):117-143.
- 526 [29] Simpson EH. Measurement of diversity. Nature 1949;163:688.
- 527 [30] Thompson JD, D. G. Higgins, and T. J. Gibson. CLUSTAL W: improving the
528 sensitivity of progressive multiple sequence alignment through sequence weighting,
529 position-specific gap penalties and weight matrix choice. Nucleic Acids Res
530 1994;22:4673-80.
- 531 [31] Hall T. BioEdit: a user-friendly biological sequence alignment editor and analysis
532 program for Windows 95/98/NT. Nucleic Acids Symp Ser 1999;41:95-98.
- 533 [32] Kimura M. A simple method for estimating evolutionary rates of base substitutions
534 through comparative studies of nucleotide sequence. J Mol Biol 1980;16:111-120.
- 535 [33] Saitou N, and M. Nei. The neighbor-joining method: a new method for reconstructing
536 phylogenetic trees. Mol Biol Evol 1987;4:406-25.
- 537 [34] Felsenstein J. Confidence-limits on phylogenies - an approach using the bootstrap.
538 Evolution 1985;39(4):783-91.

- 539 [35] Gouy M, Guindon S, Gascuel O. SeaView Version 4: A multiplatform graphical user
540 interface for sequence alignment and phylogenetic tree building. *Mol Biol Evol*
541 27(2):221-4.
- 542 [36] Tang GL, Huang J, Sun ZJ, Tang QQ, Yan CH, Liu GQ. Biohydrogen production
543 from cattle wastewater by enriched anaerobic mixed consortia: Influence of
544 fermentation temperature and pH. *J Biosci Bioeng* 2008;106(1):80-7.
- 545 [37] Wang CC, Chang CW, Chu CP, Lee DJ, Chang BV, Liao CS. Producing hydrogen
546 from wastewater sludge by *Clostridium bifermentans*. *J Biotechnol* 2003;102(1):83-
547 92.
- 548 [38] Khanal SK, Chen WH, Li L, Sung SW. Biological hydrogen production: effects of pH
549 and intermediate products. *Int J Hydrogen Energy* 2004;29(11):1123-31.
- 550 [39] Van Ginkel S, Sung SW, Lay JJ. Biohydrogen production as a function of pH and
551 substrate concentration. *Environ Sci Technol* 2001;35(24):4726-30.
- 552 [40] Fang HHP, Liu H. Effect of pH on hydrogen production from glucose by a mixed
553 culture. *Bioresour Technol* 2002;82(1):87-93.
- 554 [41] Chin HL, Chen ZS, Chou CP. Fedbatch operation using *Clostridium acetobutylicum*
555 suspension culture as biocatalyst for enhancing hydrogen production. *Biotechnol*
556 *Progr* 2003;19(2):383-8.
- 557 [42] Ying YL, Lv ZM, Min H, Cheng J. Dynamic changes of microbial community
558 diversity in a photohydrogen producing reactor monitored by PCR-DGGE. *J Environ*
559 *Sci (China)* 2008;20(9):1118-25.
- 560 [43] Tolvanen KES, Santala VP, Karp MT. [FeFe]-hydrogenase gene quantification and
561 melting curve analysis from hydrogen-fermenting bioreactor samples. *Int J Hydrogen*
562 *Energy* 2010;35(8):3433-9.

- 563 [44] Zhang HS, Bruns MA, Logan BE. Biological hydrogen production by *Clostridium*
564 *acetobutylicum* in an unsaturated flow reactor. *Water Res* 2006;40(4):728-34.
- 565 [45] Duangmanee T, Padmasiri SI, Simmons JJ, Raskin L, Sung S. Hydrogen production
566 by anaerobic microbial communities exposed to repeated heat treatments. *Water*
567 *Environ Res* 2007;79(9):975-83.
- 568 [46] Carminati D, Perrone A, Neviani E. Inhibition of *Clostridium sporogenes* growth in
569 mascarpone cheese by co-inoculation with *Streptococcus thermophilus* under
570 conditions of temperature abuse. *Food Microbiol* 2001;18(6):571-9.
- 571 [47] Schmidt O, Drake HL, Horn MA. Hitherto Unknown Fe-Fe-hydrogenase gene
572 diversity in anaerobes and anoxic enrichments from a moderately acidic fen. *Appl*
573 *Environ Microbiol* 76(6):2027-31.
- 574 [48] Calusinska M, Happe T, Joris B, Wilmotte A. The surprising diversity of clostridial
575 hydrogenases: a comparative genomic perspective. *Microbiol* 2010;156:1575-88.
- 576 [49] Vignais PM, Billoud B. Occurrence, classification, and biological function of
577 hydrogenases: An overview. *Chem Rev* 2007;107(10):4206-72.
- 578

579 **Captions to figures**

580

581 **Figure 1.** Cumulative H₂ production of mixed cultures cultivated at different initial pHs.
582 Values correspond to the average of triplicate analysis and error bars represent the standard
583 deviations. The solid and dotted lines represent the H₂ production phase and the H₂
584 consumption phase, respectively.

585

586 **Figure 2.** Relative community divergence of the CE-SSCP profiles expressed by the relative
587 Euclidean distance and based on the *hydA* genes (A) and the 16S rRNA genes (B) retrieved
588 from the mixed cultures cultivated at various initial pHs. Points correspond to mean values (n
589 = 3) and error bars to standard deviations.

590

591 **Figure 3.** Dynamics of the CE-SSCP profiles based on the *hydA* genes (A) and the 16S rRNA
592 genes (B). The CE-SSCP profiles were aligned on the basis of the common ROX internal
593 standard, and areas normalized. The x, y and z axis of each CE-SSCP profiles represent the
594 relative peak migration distance, the relative peak intensity and the timeline, respectively. A
595 representative CE-SSCP profile from the three replicates is presented for each pH.

596

597 **Figure 4.** Effect of the initial pH on the Simpson's diversity index obtained from the CE-
598 SSCP profiles based on the *hydA* genes and the 16S rRNA genes at the maximum H₂
599 production rates (A) and at the maximum H₂ production potentials (B).

600

601 **Figure 5.** Neighbor-joining phylogenetic tree of the HydA sequences (134 amino acids). The
602 Genbank accession numbers (in brackets) were obtained from the protein sequence databases.
603 The sequences obtained in this study are in bold and highlighted. Circles at the branch nodes

604 represent bootstrap confidence level percentages obtained from 1000 replicates: black circles
605 = 75-100%; white circles = 50-75%. The scale bar indicates 5% sequence divergence. The
606 *Desulfovibrio vibrio* HydA sequences were used as outgroups.

Figure 1

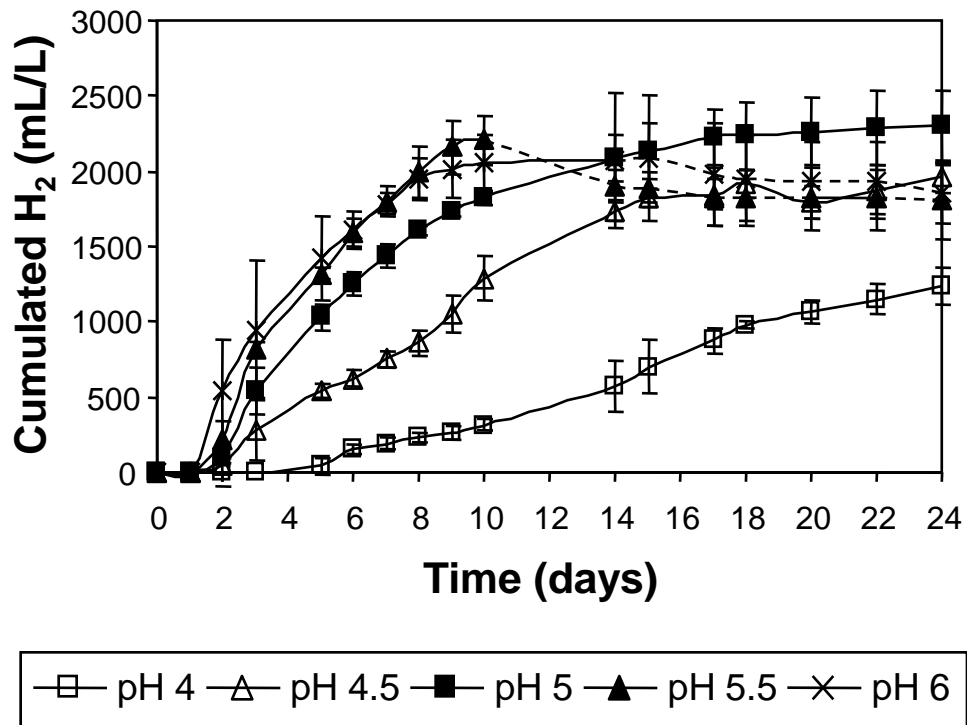
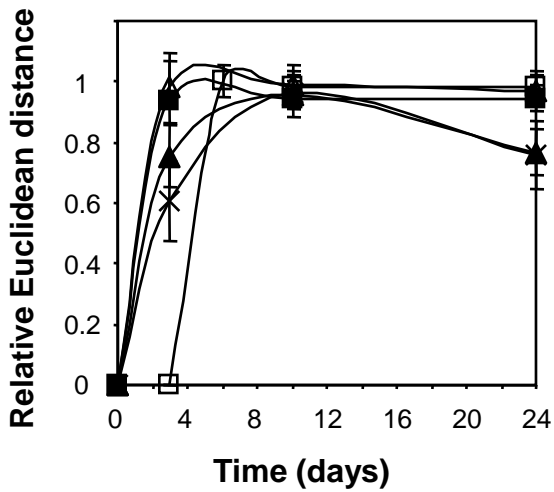
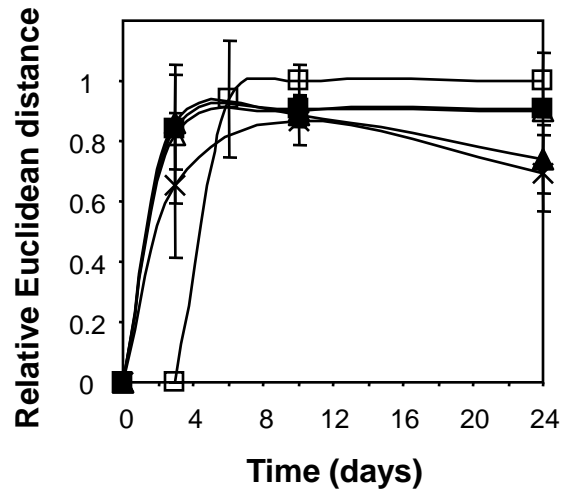


Figure 2

A. *hydA*

B. 16S rDNA



□ pH 4 △ pH 4.5 ■ pH 5 ▲ pH 5.5 × pH 6

Figure 3

Figure 3

A. *hydA*

B. 16S rDNA

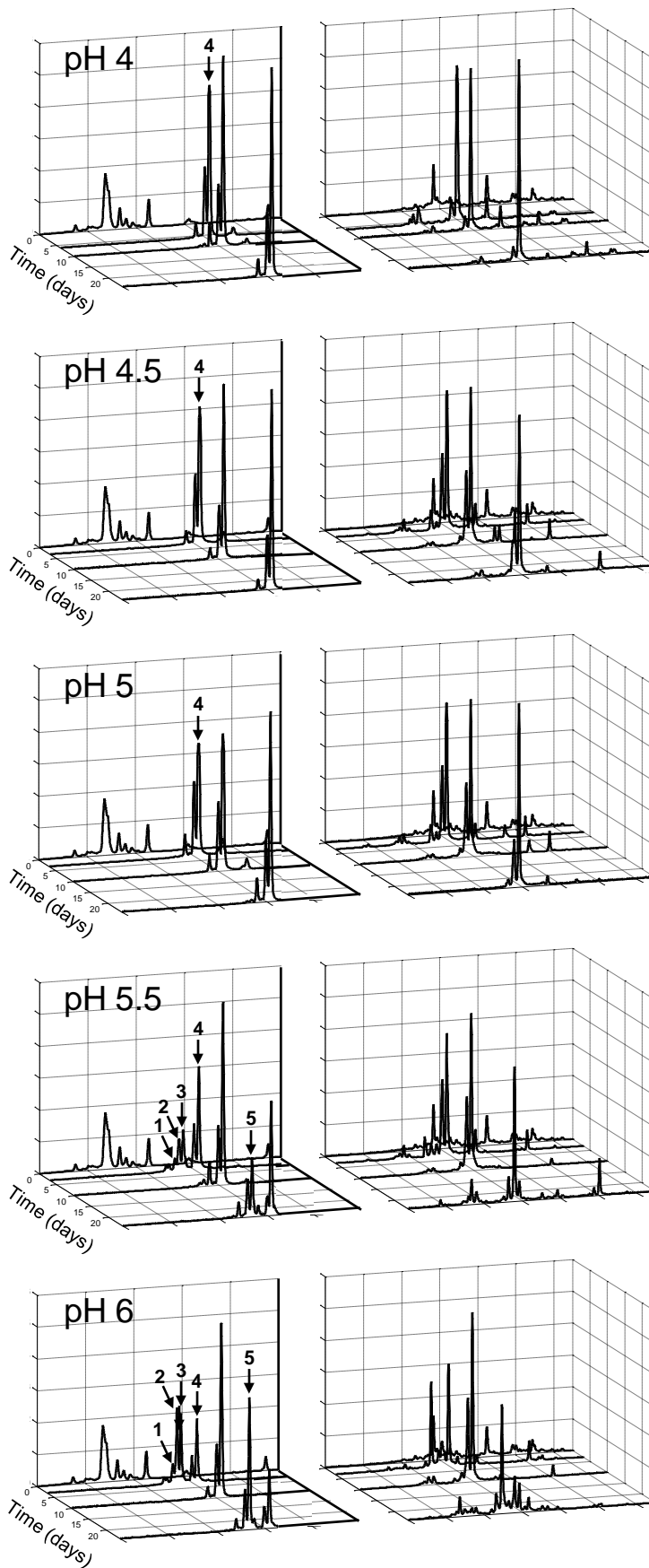


Figure 4

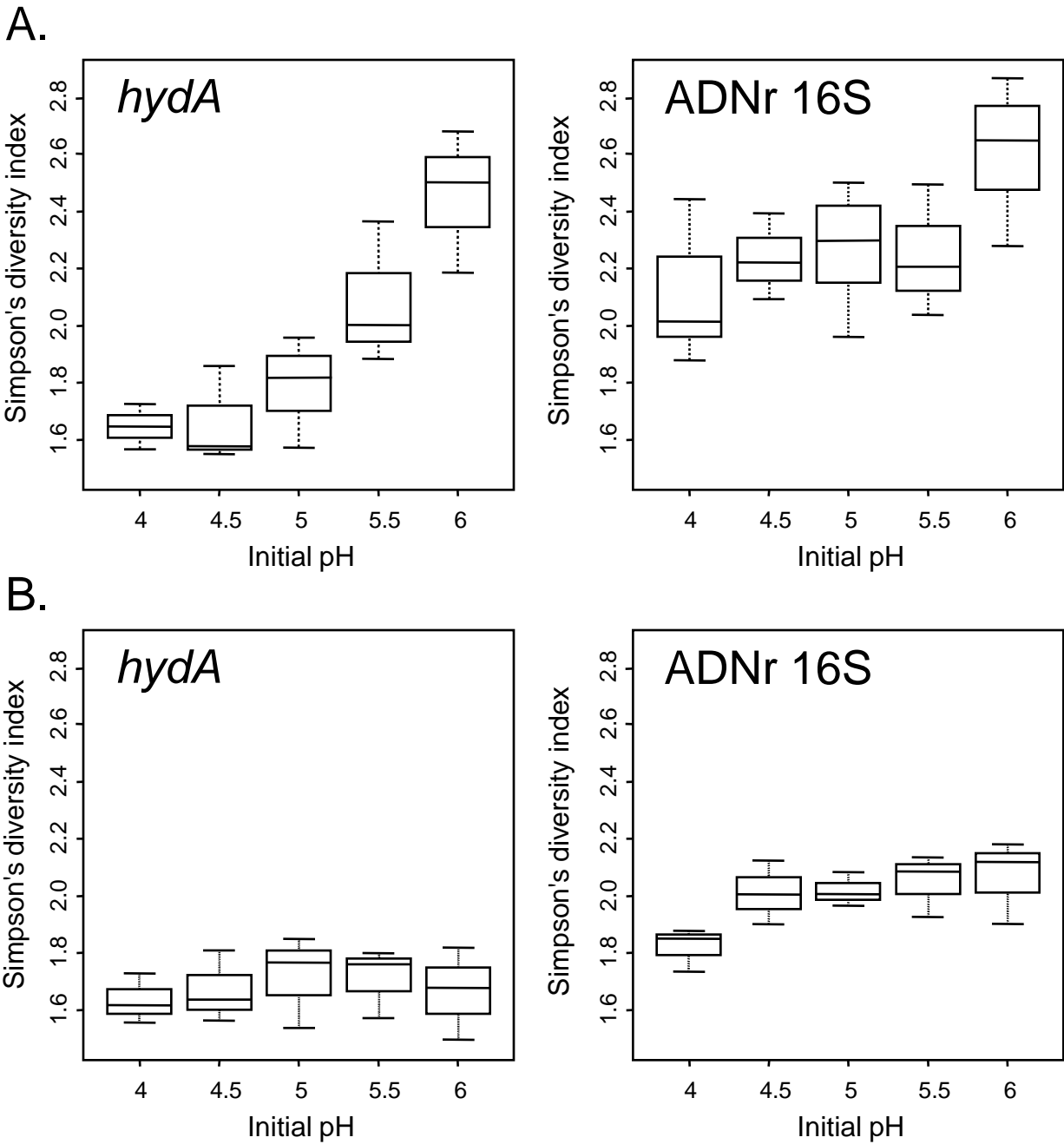


Figure 5

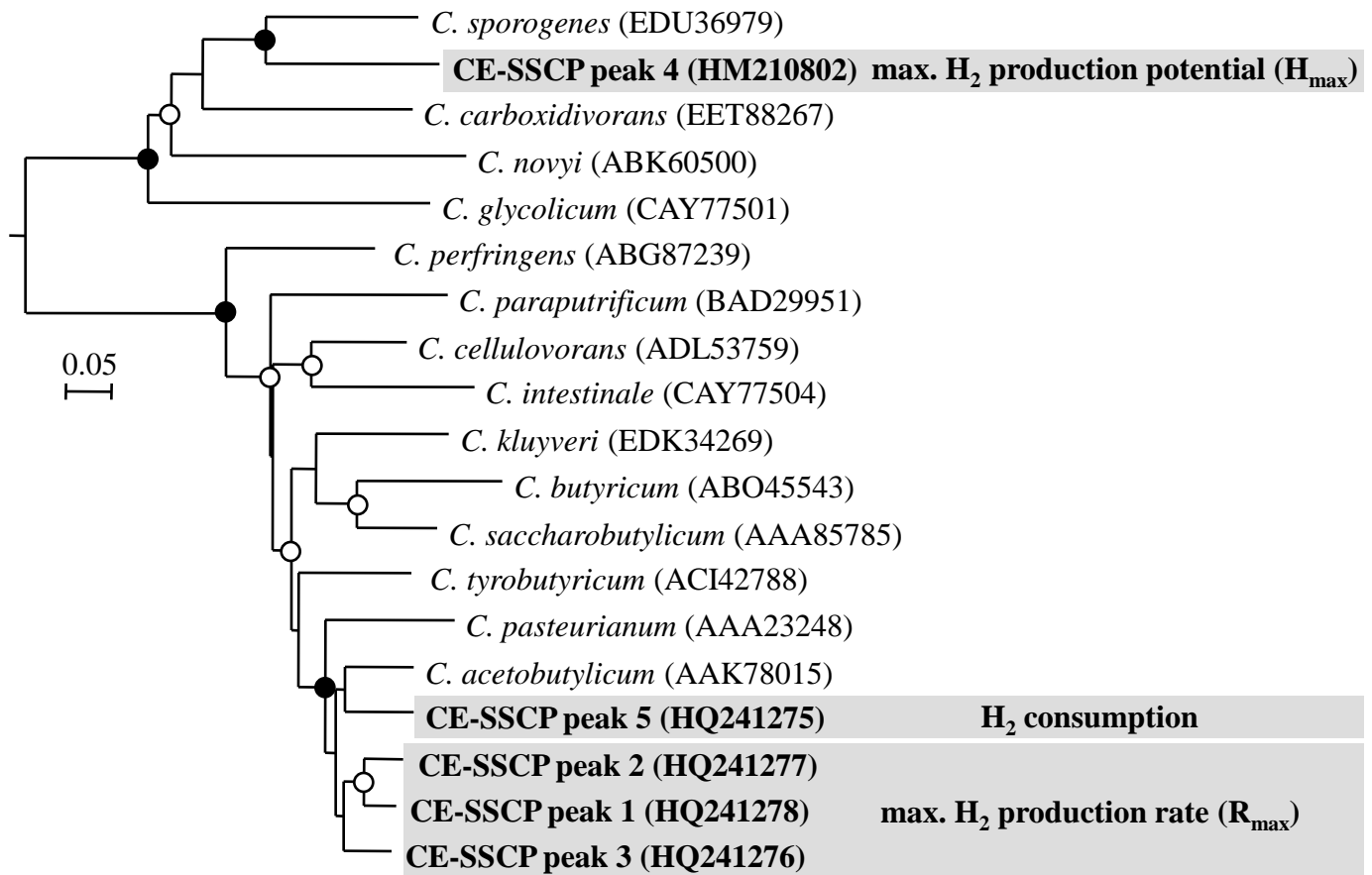


Table 1Table 1. Performance of fermentative H₂ production at different initial pH

Initial pH conditions	4	4.5	5	5.5	6	Statistical significance ²
Final pH	3.3	3.4	3.6	3.9	4.3	***
Substrate utilization (%)	53.4	75.4	94.4	99.5	100.0	***
Max. H ₂ content (%)	30.9	41.6	44.2	44.5	43.3	***
Final H ₂ content (%)	30.9	41.6	43.5	28.5	27.4	***
Max. H ₂ production rate = R _{max} (mmol-H ₂ /L/d)	16.4	20.6	24.4	28.7	38.3	***
Max. H ₂ production potential = H _{max} (mmol-H ₂ /L)	55.2	87.7	102.7	98.6	99.9	***
Max. H ₂ production potential = H _{max} (mL/L)	1237	1965	2300	2209	2238	***
Soluble microbial products = SMP (g/L) ¹	2.1	3.3	4.6	4.5	4.6	**
Volatile fatty acids = VFA (g/L) ¹	1.9	3.3	4.2	4.1	4.4	**
H ₂ yield (mol-H ₂ /mol hexose)	1.8	2.0	1.9	1.7	1.7	n.s.
Acetate yield (mol-Ac/mol hexose)	0.28	0.35	0.33	0.32	0.35	*
Butyrate yield (mol-Bu/mol hexose)	0.48	0.62	0.61	0.58	0.59	**
Ethanol yield (mol-Eth /mol hexose)	0.17	0.00	0.18	0.14	0.10	**
Bu/Ac ¹	2.5	2.6	2.7	2.7	2.5	n.s.
Final Bu/Ac	2.5	2.6	2.7	1.8	2.1	**
Time when R _{max} was reached (days)	6	3.7	3.7	3.7	3	n.s.
Time when H _{max} was reached (days)	24	24	23.3	9.7	10.3	***

¹ Values obtained when maximal H₂ production was achieved

² Significance differences between pH conditions are indicated by asterisks: *, p < 0.05; **, p < 0.005; ***, p < 5 x 10⁻⁵; n.s., not significant (p > 0.05).